Colloid Polym Sci 277:191–196 (1999)

ORIGINAL CONTRIBUTION

T. Okubo
A. Tsuchida
T. Kato

Nucleation and growth processes in the colloidal crystallization of silica spheres in the presence of sodium chloride as studied by reflection spectroscopy

Received: 15 July 1998
Accepted in revised form: 18 September 1998

T. Okubo (✉) · A. Tsuchida · T. Kato
Department of Applied Chemistry
Faculty of Engineering
Gifu University, Gifu 501-1193, Japan

Abstract Time-resolved reflection spectroscopic measurements are made for the kinetic analyses of the nucleation and growth processes of soft-type colloidal crystals of silica spheres (110 nm in diameter) in the presence of sodium chloride. Fast-scanning reflection spectra are taken using a continuous circulating-type stopped-flow cell system. The cell system is composed of a peristaltic pump and a quartz flow cell, which are connected with a PharMed tube in a closed circuit. The volume fraction of the spheres is 0.028. Induction periods range from 0.2 to 1.3 s and increase as salt concentration increases. Nucleation rates are 1×10^4 to 7×10^4 spheres/mm^{3}s anddecrease as salt concentration increases. The crystallization process has been observed from the sharpening and the increase in intensity of the reflection peaks. The crystal growth rate in the absence of salt is 23 μm/s, and decreases as salt concentration increases. The importance of electrostatic intersphere repulsion through the electrical double layers and the cooperative and synchronous fluctuation of colloidal spheres in the crystallization processes is supported.

Key words Colloidal crystal – Crystal growth kinetics – Reflection spectrum – Nucleation – Silica spheres – Salt effect

Introduction

Keen attention has been paid to the structural and dynamic properties of colloidal crystals [1–13]. Suspensions showing crystal-like structures are ideal for model studies of crystals. Furthermore, crystallization or melting phase transition phenomena occur sharply. The mechanism of colloidal crystal growth has been studied by several researchers hitherto for the two groups of colloidal crystals, i.e., diluted and deionized aqueous suspensions (''soft'' crystal) [14–20] and concentrated suspensions in refractive-index-matched organic solvents (''hard'' crystal) [21–29]. We must pay great attention to the complete deionization of the suspension especially for aqueous systems. The critical sphere concentration of melting is quite sensitive to the degree of deionization and increases sharply for suspensions contaminated with ionic impurities. When the sample suspensions are deionized with resins for more than 3 weeks, the critical concentration of melting becomes quite low and ranges from 0.0001 to 0.0003 as we have reported recently [30].

We have observed the crystallization processes of colloidal crystallization in exhaustively deionized and highly diluted aqueous suspensions from the sharpening of the reflection peak in the reflection spectra [15, 19]. The crystallization process was unexpectedly fast. In our previous papers [31–33], we studied colloidal crystallization kinetically in deionized suspensions and in organic solvents by reflection spectroscopy and dynamic light-scattering techniques. Quite recently a kinetic study on colloidal crystallization has been made in microgravity and the elongation of the induction periods corresponding to nucleation times and the lowering of

crystal growth rates have been observed [34]. In this report, colloidal crystallization kinetics has been studied for salt-containing dispersions using a cell system composed of a peristaltic pump and a quartz flow cell connected with a PharMed tube in a closed circuit. The effects of salt on the spectroscopic properties [35–38], phase diagrams [39] and other physico-chemical properties [40–51] have been studied previously.

Experimental

Materials

Colloidal silica spheres (CS-91) were a gift from Catalyst & Chemicals Ind. (Tokyo). The diameter (d_0), the standard deviation (δ) from the mean diameter, and the polydispersity index (δ/d_0) were 110 nm, 4.5 nm, and 0.041, respectively. The values of d_0 and δ were determined by electron microscopy. The charge density of the spheres was determined to be 0.48 μC/cm^2 for strongly acidic groups by conductometric titration with a Horiba model DS-14 conductivity meter. The sphere sample was carefully purified several times using an ultrafiltration cell (model 202, membrane: Diaflo-XM300, Amicon). Then the sample was treated on a mixed bed of cation- and anion-exchange resins [Bio-Rad, AG501-X8(D), 20–50 mesh] for more than 2 years before use, since newly produced silica spheres always released a considerable amount of alkali ions from the sphere surfaces for a long time. The water used for purification and for suspension preparation was purified by a Milli-Q reagent grade system (Milli-RO5 plus and Milli-Q plus, Millipore, Bedford, Mass).

Reflection spectroscopy

The cell system for the reflection spectrum measurements consists of a quartz observation cell ($40 \times 10 \times 2$ mm), a column of cation- and anion-exchange resins (Bio-Rad), and a peristaltic pump (Masterflex 7524-10, Illinois). The pump pumps the colloidal suspensions to the observation flow cell. The flow rate was 9 ml/min before the start of the measurement. A light beam from a halogen lamp (Hayashi LA-150SX, Tokyo) hits the cell wall using a Y-type optical fiber cable and the reflected light is measured on a photo-multichannel analyzer system (PMA-50, Hamamatsu Photonics, Hamamatsu). Spectra (100–250) were taken in scanning times from 5 s to 8 min. Experimental errors in the measurements are estimated to be rather large at 10%. This is due to the fact that the concentration of sodium chloride in the observation cell system was kept extremely low, of the order of 10^{-6} M.

The size of the colloidal single crystals from homogeneous nucleation, L, may be estimated by Scherrer's equation from the half-width of the reflection spectra [52–54]:

$$L \propto n\Delta q^{-1} \quad , \tag{1}$$

where n is the number of the order in the Bragg equation, q is the scattering vector, and Δq denotes $q_l - q_s$, with q_l and q_s referring to the largest and smallest wavelengths corresponding to the half-width of the reflection peak. It should be noted here that Eq. (1) is derivable by assuming a powder-like random distribution of a large number of colloidal crystals in the reflection volume. However, this assumption is difficult to accept for colloidal crystals, since the most dense planes of the colloidal single crystals tend to orient parallel to the cell plane.

On the other hand, the peak intensity, I, of the reflection spectra is approximated by Eq. (2) [54],

$$I \propto N_{\mathrm{cryst}} L^3 \propto L^3 \quad , \tag{2}$$

where N_{cryst} is the number of single crystals in the reflecting volume, which is directly proportional to the number concentration of crystals in the final stages of the crystallization process, being equal to the total number of nuclei which were formed in the whole course of crystallization.

Results and discussion

Time-resolved reflection spectra

Typical reflection spectra in the course of crystallization are shown in Fig. 1 in the presence of sodium chloride (5×10^{-6} M) at a volume fraction $\phi = 0.028$. The spectra were taken every 500 ms. The reflection peak became sharp with time in the course of crystallization, and this corresponds to an increase in crystal size. The background intensity decreased slightly in the course of crystallization, though this is not clear in Fig. 1. This decrease is ascribed to the decrease in the multiple scattering of the suspension. The reflection spectra sharpened further and their intensities increased when the measurements were made for long periods (470 s).

An example of the time dependencies of the peak wavelengths (λ_p) is shown in Fig. 2. A short period after stopping the suspension flow the broad peak appeared first in a higher wavelength region. The peaks then sharpened and their wavelengths decreased. This supports the fact that metastable and expanded structures are formed first and then the crystals become more stable and more dense.

Figure 3 shows the λ_p values as a function of salt concentration. Though the experimental errors were

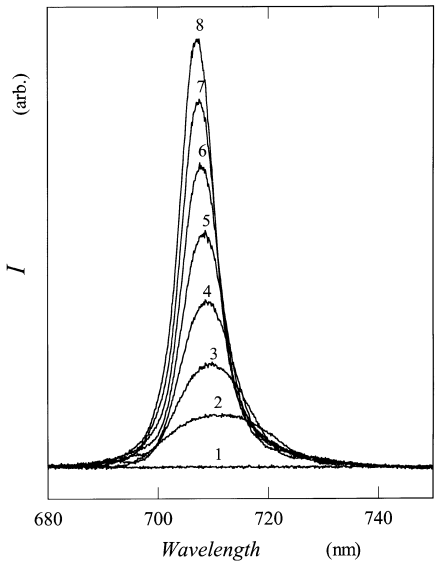

Fig. 1 Reflection spectra in the course of crystallization of CS-91 spheres in the presence of sodium chloride at 25 °C. Volume fraction $\phi = 0.028$, [NaCl] $= 5 \times 10^{-6}$ M. Curve *1*: 0 s after stopping the flow, *2*: 0.5 s, *3*: 1 s, *4*: 1.5 s, *5*: 2 s, *6*: 2.5 s, *7*: 3.5 s, *8*: 4.5 s

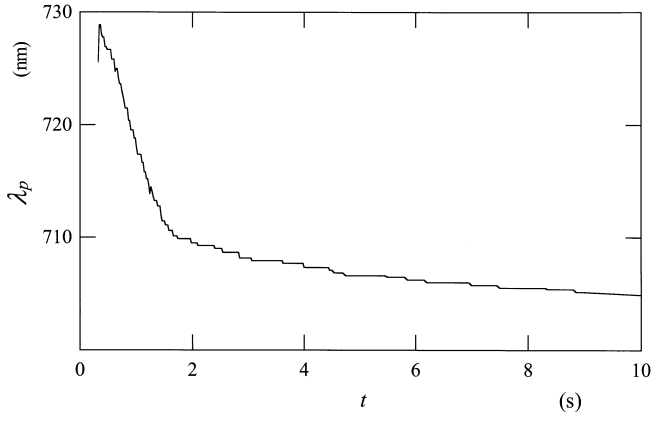

Fig. 2 Peak wavelengths in the course of colloidal crystallization of CS-91 spheres in the presence of sodium chloride at 25 °C. $\phi = 0.028$, [NaCl] $= 5 \times 10^{-6}$ M

rather large, the peak wavelength decreased as the concentration of sodium chloride increased. This tendency is explained by the salt effect of thinning the electrical double layers surrounding the colloidal spheres. The region where simple ions distribute is called the electrical double layer. The thickness of the electrical double layer is approximated by the Debye screening length, l_{DH} given by Eq. (3).

$$l_{DH} = (4\pi e^2 n/\varepsilon k_B T)^{-1/2} \quad , \tag{3}$$

where, e is the electronic charge and ε is the dielectric constant of the solvent. n is the concentration of

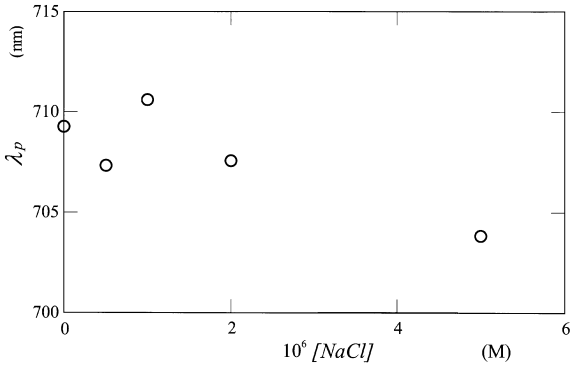

Fig. 3 Equilibrium peak wavelengths in the course of crystallization of CS-91 spheres at 25 °C. $\phi = 0.028$, [NaCl] $= 5 \times 10^{-6}$ M

"diffusible" or "free-state" cations and anions in suspension. Thus, n is the sum of the concentration of diffusible counterions (n_c), foreign salt (n_s), and both H^+ and OH^- from the dissociation of water (n_o), i.e. $n = n_c + n_s + n_o$. In this work n_o was taken to be 2×10^{-7} (mol/l) $\times N_A \times 10^{-3}$ cm^{-3}, where N_A is Avogadro's number. In order to estimate n_c, the fraction of free counterions (β) must be known. Values of β have been determined for many kinds of colloidal spheres of various sizes and charge densities [55–58]. The total stoichiometric number of charges on a sphere is the only factor needed to determine β. β for CS91 spheres was estimated to be 0.1. The estimated l_{DH} values were 153 nm, 125 nm, and 108 nm for the colloidal crystals containing 0 μM, 2 μM, and 4 μM sodium chloride, respectively. The effective diameters, $l_{eff} = d_0 + 2l_{DH}$, of CS91 spheres are estimated to be 417 nm, 359 nm, and 326 nm, respectively. On the other hand, the mean nearest neighbor intersphere distance, l_0, is 328 nm irrespective of salt concentration. Following the effective soft-sphere model, when $l_{eff} > l_0$, crystal-like ordering should occur. Comparing the l_{eff} values with l_0, the relation $l_{eff} > l_0$ always holds, though l_{eff} decreases as the salt concentration increases. It should be noted that the relationship between λ_p and the nearest neighbor intersphere distance observed, l, is given by Eq. (4) [35].

$$l = 0.4595\lambda_p, \quad \text{at 25 °C in water} \tag{4}$$

Thus, our calculation supports the validity of the idea of the effective soft-sphere model and also the tendency of λ_p to decrease with increasing salt concentration.

An example trace of the intensities of the reflection peaks in the course of colloidal crystallization is shown in Fig. 4: the S-shaped characteristic is clear. A short induction period (t_i) was also observed in the salt-containing system. These features are the same as those of the deionized systems.

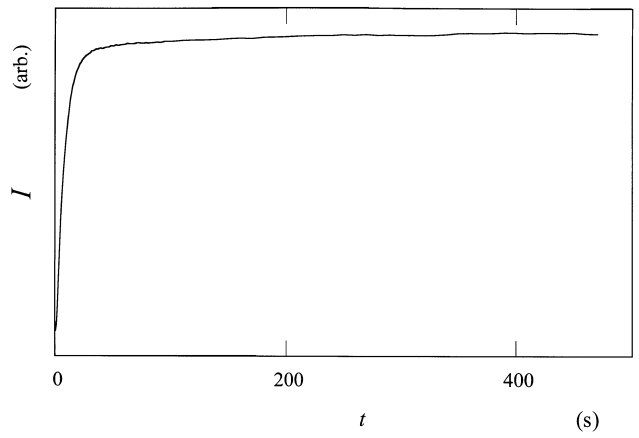

Fig. 4 Reflection peak intensities in the course of colloidal crystallization of CS-91 spheres in the presence of sodium chloride at 25 °C

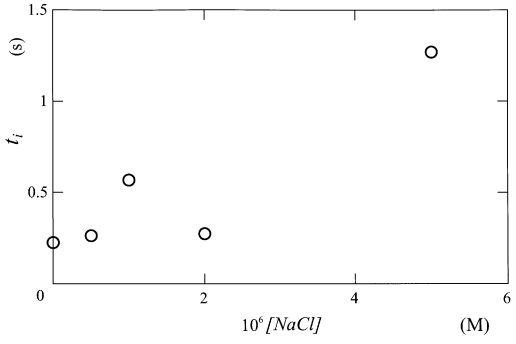

Fig. 5 Induction periods in the colloidal crystallization of CS-91 spheres at 25 °C. $\phi = 0.028$

Nucleation process

Figure 5 shows the induction time (t_i) observed in this work. t_i ranged from 0.2 to 1.3 s and increased as the concentration of sodium chloride increased.

Most kinetic measurements on colloidal crystallization, including this work, have observed an induction period, after which crystal growth started especially in dilute suspensions. This observation suggests that the kinetics of colloidal crystallization is explainable by classical diffusive crystallization theory including nucleation and crystal growth processes.

The number of nuclei that germinate per unit time, the nucleation rate, v_n, is given by

$$v_n = N_n/t_i \ , \tag{5}$$

where N_n is the total number of nuclei which are formed during the nucleation process and t_i is the induction period. Here, we assume that the number of nuclei equals the number of single crystals formed. The number of sphere particles per mean size of single crystal, N_c for a cubic lattice is given by

$$N_c = \sqrt{2}L^3/l^3 \ , \tag{6}$$

where L and l are the mean size of single crystals formed and the closest intersphere distance, respectively. The total number of colloidal spheres (N_T) in a unit volume is $\phi/[(4/3)\pi(d_0/2)^3]$. Then v_n is given by Eq. (7)

$$v_n = N_T/N_c t_i = \phi l^3/[(4\sqrt{2}/3)\pi(d_0/2)^3 L^3 t_i] \ . \tag{7}$$

The l value is given by Eq. (8)

$$l = 0.904 d_0 \phi^{-1/3} \ . \tag{8}$$

The mean size of single crystals formed was estimated by close-up photographs to be 40 μm irrespective of salt concentration. v_n values were thus estimated to be 69 000, 59 000, 57 000, and 12 000 spheres/mm^{3}s at [NaCl] = 0, 0.5, 2, and 5 μM, respectively. Though the experimental errors were rather large, v_n decreased as the salt concentration increased. The electrostatic intersphere repulsion must decrease when salt is added in suspension. The apparent attraction between spheres, which is induced by the difference between the repulsive forces in the nuclei and liquid regions as will be discussed later, should then decrease. Thus, a decrease in nucleation rate should result.

It should be mentioned here that the size of single crystals is polydisperse as has been observed previously [35]. Therefore, the clear-cut separation of the nucleation step from the crystallization process will be difficult, and the nucleation reaction may remain even in the crystal growth period. It should also be mentioned that Ostwald ripening of the crystals, i.e., further growth of large crystals and disappearance of small ones, was not observed for our colloidal crystallization systems.

Crystal growth process

The crystal sizes determined from the half-width method using Eq. (1) are shown in Fig. 6 as a function of time. Clearly, after the induction period crystal size increased linearly at the beginning of the crystal growth process. The crystal growth rate was evaluated from the slope. Figure 7 shows a typical example of the cube root of the reflection peak intensities given in Fig. 4 against time plots. Crystal sizes were also estimated using Eq. (2) and the final average size of the single crystals formed.

According to Wilson [59] and Frenkel [60], the crystal growth rate of a crystal, v, is given by

$$v = v_\infty[1 - \exp(-\Delta\mu/k_B T)] \ . \tag{9}$$

Here, $\Delta\mu$ is the chemical potential difference between the crystal and liquid phases and is given by Eq. (10)

$$\Delta\mu = \mu_{cryst} - \mu_{liq} \ . \tag{10}$$

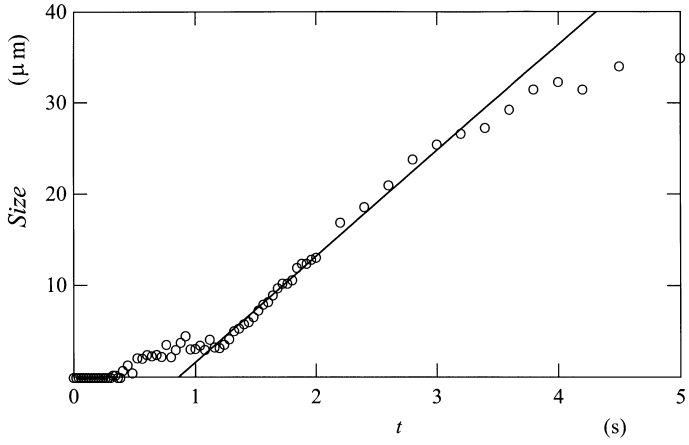

Fig. 6 Crystal size estimated from the half-width method in the course of crystallization of CS-91 spheres at 25 °C. $\phi = 0.028$, $[NaCl] = 5 \times 10^{-6}$ M

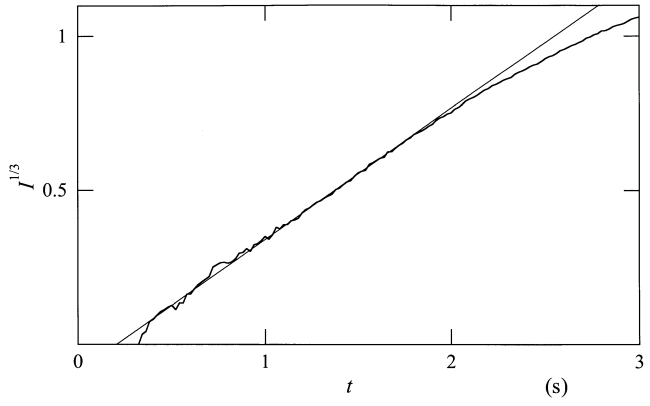

Fig. 7 Cube roots of the reflection intensity in the course of crystallization of CS-91 spheres at 25 °C. $\phi = 0.028$, $[NaCl] = 5 \times 10^{-6}$ M

$\Delta\mu > 0$ means that crystallization will proceed. We should note that Eq. (11) holds [61].

$$\Delta\mu/k_B T = \ln(\phi/\phi_c) \cong \sigma \ , \tag{11}$$

where σ is the relative super-saturation given by $(\phi - \phi_c)/\phi_c$. From Eqs. (9) and (11), Eq. (12) is derived

$$v = v_\infty[1 - \exp(-\sigma)] \ , \tag{12}$$

Equation (12) is further simplified as

$$v = v_\infty - v_\infty \phi_c/\phi \ . \tag{13}$$

Figure 8 shows the salt effect on the crystal growth rates evaluated from the half-width and the cube root methods. Clearly, the rates decreased as the concentration of sodium chloride increased. The main causes for the retardation effect by the salt is ascribed to the thinning of the electrical double layers and the decrease

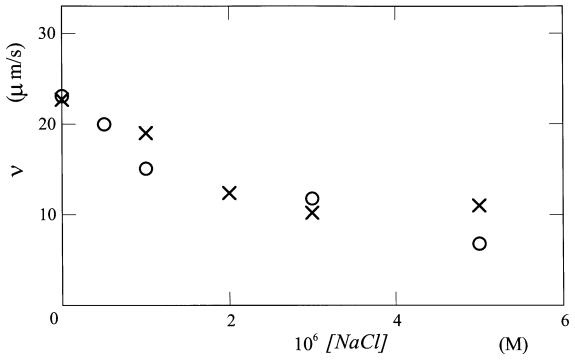

Fig. 8 Crystal growth rates, v_∞, as a function of reciprocal sphere concentration estimated from the half-width (O) and peak intensity methods (X) at 25 °C. $\phi = 0.028$

of electrostatic intersphere repulsive forces. The importance of the thinning effect of the electrical double layers is, therefore, clear for the experimental results for the decrease in the nucleation and crystal growth processes as discussed in the previous section.

Importance of intersphere repulsion and the synchronous fluctuation of colloidal spheres in crystallization

The critical concentration of melting (ϕ_c) of the colloidal crystals in the exhaustively deionized state is very low (volume fraction around 0.0002 in most cases) as described in the Introduction. However, the effective concentration of spheres including the expanded electrical double layers is substantially higher even close to a volume fraction of 0.74 corresponding to close packing. Each sphere in the colloidal crystals interacts very strongly and furthermore in a cooperative manner through the electrical double layers by electrostatic repulsion. Recently, Schatzel and Ackerson [27] proposed the importance of the dynamic phase transition by density fluctuation in colloidal crystallization. It should be noted that the synchronous fluctuation of colloidal spheres in the crystal cages plays an important role in colloidal crystallization. The importance of the dynamic phase transition has been reported for other crystals such as metals [62] and polymers [63].

Many researchers including Hachisu et al. have clarified the importance of the electrostatic repulsive forces between spheres in colloidal crystal systems [64, 65]. The intersphere repulsion should also exist in the course of crystallization including nucleation and growth. The electric double layers for the colloidal crystals are more expanded compared with those of colloidal liquids [37, 66]. This situation means that the microscopic intersphere repulsion forces in the colloidal crystals are weak though very slightly compared with those of colloidal liquids. Therefore, there should be an

"apparent" intersphere "attraction" in the course of the nucleation and growth processes in the phase transition from liquids to crystals. In other words, the slight difference in the repulsive forces in the crystals and the liquids leads to apparent attraction between spheres in the nucleus regions. This apparent attraction in colloidal crystallization processes must be one of the main reasons why the kinetic and morphological properties of colloidal crystals are so similar to those of other crystal systems such as metals, protein crystals, and minerals. Among the many crystal systems, crystallization of fused metals will be one of the best systems to mimic colloidal crystals. It should also be mentioned that only intersphere repulsion exists in the course of colloidal crystallization, and there are actually never any attractive forces. The authors believe strongly that the origin of the synchronous fluctuation of colloidal spheres in the course and/or in the completed crystallization is the repulsive interaction itself.

Acknowledgements This work was supported by a grant-in-aid from the Japan Space Utilization Promotion Center. M. Komatsu and M. Hirai of Catalysts & Chemicals Ind. (Tokyo) are thanked for providing the silica samples.

References

1. Vanderhoff W, van de Hul HJ, Tausk RJM, Overbeek JThG (1970) In: Goldfinger G (ed) Clean surfaces: their preparation and characterization for interfacial studies. Dekker, New York, pp 15–44
2. Hiltner PA, Papir YS, Krieger IM (1971) J Phys Chem 75:1881
3. Kose A, Ozaki M, Takano K, Kobayashi Y, Hachisu S (1973) J Colloid Interface Sci 44:330
4. Williams R, Crandall RS, Wojtowicz PJ (1976) Phys Rev Lett 37:348
5. Mitaku S, Ohtsuki T, Enari K, Kishimoto A, Okano K (1978) Jpn J Appl Phys 17:305
6. Lindsay HM, Chaikin PM (1982) J Chem Phys 76:3774
7. Pieranski P (1983) Contemp Phys 24:25
8. Ottewill RH (1985) Ber Bunsenges Phys Chem 89:517
9. Aastuen DJW, Clark NA, Cotter LK, Ackerson BJ (1986) Phys Rev Lett 57:1733
10. Pusey PN, van Megen W (1986) Nature 320:340
11. Okubo T (1988) Acc Chem Res 21:281
12. Russel WB, Saville DA, Schowalter WR (1989) Colloidal dispersions. Cambridge University Press, Cambridge, UK
13. Sood AK (1991) Solid State Phys 45:2
14. Ackerson BJ, Clark NA (1981) Phys Rev Lett 46:123
15. Okubo T (1988) J Chem Soc Faraday Trans 1 84:1163
16. Aastuen DJW, Clark NA, Swindal JC, Muzny CD (1990) Phase Transition 21:139
17. Lowen H, Palberg T, Simon R (1993) Phys Rev Lett 70:1557
18. Grier DG, Murray CA (1994) J Chem Phys 100:9088
19. Okubo T (1994) In: Macro-ion characterization. From dilute solutions to complex fluids. ACS Symp Ser 548. ACS, Washington, DC, pp 364–380
20. Wurth N, Schwarz J, Culis F, Leidener P, Palberg T (1995) Phys Rev E 52:6415
21. Pusey PN, van Megen W (1987) In: Safran SA, Clark NA (eds) Complex and supramolecular fluids. Wiley Interscience, New York, pp 673–698
22. Davis KE, Russel WB (1988) Ceram Trans B 1:693
23. Russel WB (1990) Phase Transitions 21:127
24. Harkless CR, Singh MA, Nagler SE, Stephenson GB, Jordan-Sweet JL (1990) Phys Rev Lett 64:2285
25. Dhont JKG, Smits C, Lekkerkerker HNW (1992) J Colloid Interface Sci 152:386
26. Schatzel K, Ackerson BJ (1992) Phys Rev Lett 68:337
27. Schatzel K, Ackerson BJ (1993) Phys Rev E 48:3766
28. Verhaegh NAM, van Blaaderen A (1994) Langmuir 10:1427
29. Butler S, Harrowell P (1995) Phys Rev E 52:6424
30. Okubo T (1994) Langmuir 10:1695
31. Okubo T, Okada S, Tsuchida A (1997) J Colloid Interface Sci 189:337
32. Okubo T, Okada S (1997) J Colloid Interface Sci 192:490
33. Okubo T, Okada S (1998) J Colloid Interface Sci 204:198
34. Okubo T, Tsuchida A, Okuda T, Fujitsuna K, Ishikawa M, Morita T, Tada T (1998) Colloids Surf (in press)
35. Okubo T (1986) J Chem Soc Faraday Trans 1 82:3163
36. Okubo T (1986) J Chem Soc Faraday Trans 1 82:3185
37. Okubo T (1990) J Chem Soc Faraday Trans 86:2871
38. Okubo T (1992) Ber Bunsenges Phys Chem 96:61
39. Okubo T, Fujita H, Kiriyama K, Yamaoka H (1996) Colloid Polym Sci 274:73
40. Okubo T (1987) J Chem Phys 86:5182
41. Okubo T (1987) Colloid Polym Sci 265:522
42. Okubo T (1987) J Chem Phys 87:6733
43. Okubo T (1988) Naturwissenschaften 75:91
44. Okubo T (1988) J Chem Phys 88:6581
45. Okubo T (1988) Ber Bunsenges Phys Chem 92:504
46. Matsumoto T, Okubo T (1991) J Rheol 35:135
47. Okubo T (1994) J Chem Phys 98:1472
48. Okubo T, Kiriyama K, Yamaoka H, Nemoto N (1995) Colloids Surf 103:47
49. Okubo T (1995) J Chem Phys 102:7721
50. Okubo T, Kiriyama K, Nemoto N, Hashimoto H (1996) Colloid Polym Sci 274:93
51. Okubo T, Kiriyama K (1996) Ber Bunsenges Phys Chem 100:849
52. James RW (1965) In: L Bragg (ed) The optical principles of the diffraction of X-rays. The crystal state, vol II. Cornell University Press, Ithaca, NY
53. Okubo T (1986) J Chem Soc Faraday Trans 1 82:3163
54. Dhont JKG, Smits C, Lekkerkerker HNW (1992) J Colloid Interface Sci 152:386
55. Schaefer DW (1977) J Chem Phys 66:3980
56. Alexander S, Chaikin PM, Grant P, Morales GJ, Pincus P, Hone D (1984) J Chem Phys 80:5776
57. Okubo T (1987) Ber Bunsenges Phys Chem 91:1064
58. Okubo T (1988) J Colloid Interface Sci (1988) 125:380
59. Wilson HA (1900) Philos Mag 50:238
60. Frenkel J (1932) Phys Z Sowjetunion 1:498
61. Hartman P (ed) (1973) Crystal growth. An introduction. North-Holland, Amsterdam
62. Fujita H (1988) Proceedings of the 4th Asia-Pacific Conference Workshop on Electron Microscopy, p 215
63. Imai M, Mori K, Mizukami T, Kaji K, Kanaya T (1992) Polymer 33:4451
64. Okubo T (1993) Prog Polym Sci 18:481
65. Okubo T (1996) Colloids Surf A 109:77
66. Arora AK, Tata BVR, Sood AK, Kasavana R (1988) Phys Rev Lett 60:2438